arXiv:cond-mat/0310378v1 16 Oct 2003

A FOURTH-ORDER TIME-SPLITTING LAGUERRE-HERMITE PSEUDO-SPECTRAL METHOD FOR BOSE-EINSTEIN CONDENSATES

WEIZHU BAO * AND JIE SHEN †

Abstract. A fourth-order time-splitting Laguerre-Hermite pseudospectral method is introduced for Bose-Einstein condensates (BEC) in 3-D with cylindrical symmetry. The method is explicit, unconditionally stable, time reversible and time transverse invariant. It conserves the position density, and is spectral accurate in space and fourth-order accurate in time. Moreover, the new method has two other important advantages: (i) it reduces a 3-D problem with cylindrical symmetry to an effective 2-D problem; (ii) it solves the problem in the whole space instead of in a truncated artificial computational domain. The method is applied to vector Gross-Pitaevskii equations (VGPEs) for multi-component BECs. Extensive numerical tests are presented for 1-D GPE, 2-D GPE with radial symmetry, 3-D GPE with cylindrical symmetry as well as 3-D VGPEs for two-component BECs to show the efficiency and accuracy of the new numerical method.

Key words. Gross-Pitaevskii equation (GPE), Bose-Einstein condensate (BEC), time-splitting, Laguerre-Hermite pseudospectral method, Vector Gross-Pitaevskii equations (VGPEs).

AMS subject classifications. 35Q55, 65T99, 65Z05, 65N12, 65N35, 81-08

1. Introduction.

Since its realization in dilute bosonic atomic gases [3, 13], Bose-Einstein condensation of alkali atoms and hydrogen has been produced and studied extensively in the laboratory [26], and has spurred great excitement in the atomic physics community and renewed the interest in studying the collective dynamics of macroscopic ensembles of atoms occupying the same one-particle quantum state [32, 18, 24]. Theoretical predictions of the properties of a BEC like the density profile [12], collective excitations [21] and the formation of vortices [34] can now be compared with experimental data [3]. Needless to say that this dramatic progress on the experimental front has stimulated a wave of activity on both the theoretical and the numerical front.

The properties of a BEC at temperatures T much smaller than the critical condensation temperature T_c [29] are usually well modeled by a nonlinear Schrödinger equation (NLSE), also called Gross-Pitaevskii equation (GPE) [29, 33], for the macroscopic wave function which incorporates the trap potential as well as the interactions among the atoms. The effect of the interactions is described by a mean field which leads to a nonlinear term in the GPE. The cases of repulsive and attractive interactions - which can both be realized in the experiment - correspond to defocusing and focusing nonlinearities in the GPE, respectively. The results obtained by solving the GPE showed excellent agreement with most of the experiments (for a review see [4, 17]). In fact, up to now there have been very few experiments in ultra-cold dilute bosonic gases which could not be described properly by using theoretical methods based on the GPE [23, 28]. Thus developing efficient numerical methods for solving GPE is very important in numerical simulation of BEC.

*Department of Computational Science, National University of Singapore, Singapore 117543 (*bao@cz3.nus.edu.sg*). URL: http://www.cz3.nus.edu.sg/~bao/. Research is supported by the National University of Singapore grant No. R-151-000-027-112.

†Department of Mathematics, Purdue University, West Lafayette, IN 47907, USA, (*shen@math.purdue.edu*). Research is supported by NSF DMS-0311915 and he acknowledges support by the OAP (Fellow-Inbound) Programme supported by A*STAR and National University of Singapore.

Recently, a series of numerical studies are devoted to the numerical solution of time-independent GPE for finding the ground states and of time-dependent GPE for determining the dynamics of BECs. To compute ground states of BECs, Bao and Du [6] presented a continuous normalized gradient flow (CNGF) with diminishing energy, and discretized it by a backward Euler finite difference (BEFD) method; Bao and Tang [9] proposed a method which can be used to compute the ground and excited states via directly minimizing the energy functional; Edwards and Burnett [20] introduced a Runge-Kutta type method; other methods include an explicit imaginary-time algorithm in [1, 16]; a directly inversion in the iterated subspace (DIIS) in [36] and a simple analytical type method in [19]. To determine the dynamics of BECs, Bao et al. [10, 5, 11] presented a time-splitting spectral (TSSP) method, Ruprecht et al. [35] used the Crank-Nicolson finite difference (CNFD) method, Cerimele et al. [14, 15] proposed a particle-inspired scheme.

In most experiments of BECs, the magnetic trap is with cylindrical symmetry. Thus, the 3-D GPE in Cartesian coordinate can be reduced to an effective 2-D problem in cylindrical coordinate. In this case, both the TSSP [10, 11, 5] and CNFD [35] methods have serious drawbacks: (i) One needs to replace the original whole space by a truncated computational domain with an artificial (usually homogeneous Dirichlet boundary conditions are used) boundary condition. How to choose an appropriate bounded computational domain is a difficult task in practice: if it is too large, the computational resource is wasted; if it is too small, boundary effect will lead to wrong numerical solutions. (ii) The TSSP method is explicit and of spectral accuracy in space, but one needs to solve the original 3-D problem due to the periodic/homogeneous Dirichlet boundary conditions required by Fourier/sine spectral method. Thus, the memory requirement is a big burden in this case. The CNFD discretizes the 2-D effective problem directly, but it is implicit and only second-order accurate in space. The aim of this paper is to develop a numerical method which enjoys advantages of both TSSP and CNFD. That is to say, the method is explicit and of spectral order accuracy in space, and discretizes the effective 2-D problem directly. We shall present such an efficient and accurate numerical method for discretizing 3-D GPE with cylindrical symmetry by applying a time-splitting technique and constructing appropriately scaled Laguerre-Hermite basis functions.

The paper is organized as follows. In Section 2, we present the Gross-Pitaevskii equation and its dimension reduction. In Section 3, we present time-splitting Hermite, Laguerre and Laguerre-Hermite spectral methods for 1-D GPE, 2-D GPE with radial symmetry and 3-D GPE with cylindrical symmetry, respectively. Extension of the time-splitting Laguerre-Hermite spectral method for vector Gross-Pitaevskii equations (VGPEs) for multi-component BEC is presented in Section 4. In Section 5, numerical results for 1-D GPE, 2-D GPE with radial symmetry, 3-D GPE with cylindrical symmetry as well as 3-D VGPEs for multi-component BEC are reported to demonstrate the efficiency and accuracy of our new numerical methods. Some concluding remarks are given in Section 6.

2. The Gross-Pitaevskii equation (GPE). At temperatures T much smaller than the critical temperature T_c [29], a BEC is well described by the macroscopic wave function $\psi = \psi(\mathbf{x}, t)$ whose evolution is governed by a self-consistent, mean field nonlinear Schrödinger equation (NLSE) known as the Gross-Pitaevskii equation (GPE) [25, 33]

$$i\hbar\frac{\partial\psi(\mathbf{x},t)}{\partial t} = -\frac{\hbar^2}{2m}\nabla^2\psi(\mathbf{x},t) + V(\mathbf{x})\psi(\mathbf{x},t) + NU_0|\psi(\mathbf{x},t)|^2\psi(\mathbf{x},t), \tag{2.1}$$

where m is the atomic mass, $\hbar$ is the Planck constant, N is the number of atoms in the condensate, $V(\mathbf{x})$ is an external trapping potential. When a harmonic trap potential is considered, $V(\mathbf{x}) = \frac{m}{2}\left(\omega_x^2 x^2 + \omega_y^2 y^2 + \omega_z^2 z^2\right)$ with ω_x, ω_y and ω_z being the trap frequencies in x, y and z-direction, respectively. In most current BEC experiments, the traps are cylindrically symmetric, i.e. $\omega_x = \omega_y$. $U_0 = 4\pi\hbar^2 a_s/m$ describes the interaction between atoms in the condensate with the s-wave scattering length a_s (positive for repulsive interaction and negative for attractive interaction). It is convenient to normalize the wave function by requiring

$$\int_{\mathbb{R}^3} |\psi(\mathbf{x},t)|^2 \, d\mathbf{x} = 1. \tag{2.2}$$

2.1. Dimensionless GPE. In order to scale the Eq. (2.1) under the normalization (2.2), we introduce

$$\tilde{t} = \omega_m t, \quad \tilde{\mathbf{x}} = \frac{\mathbf{x}}{a_0}, \quad \tilde{\psi}(\tilde{\mathbf{x}},\tilde{t}) = a_0^{3/2}\psi(\mathbf{x},t), \quad \text{with} \quad a_0 = \sqrt{\hbar/m\omega_m}, \tag{2.3}$$

where $\omega_m = \min\{\omega_x, \omega_y, \omega_z\}$, a_0 is the length of the harmonic oscillator ground state. In fact, we choose $1/\omega_m$ and a_0 as the dimensionless time and length units, respectively. Plugging (2.3) into (2.1), multiplying by $1/m\omega_m^2 a_0^{1/2}$, and then removing all $\tilde{}$, we get the following dimensionless GPE under the normalization (2.2) in three dimension

$$i\,\frac{\partial\psi(\mathbf{x},t)}{\partial t} = -\frac{1}{2}\nabla^2\psi(\mathbf{x},t) + V(\mathbf{x})\psi(\mathbf{x},t) + \beta\,|\psi(\mathbf{x},t)|^2\psi(\mathbf{x},t), \tag{2.4}$$

where $\beta = \frac{U_0 N}{a_0^3\hbar\omega_m} = \frac{4\pi a_s N}{a_0}$ and

$$V(\mathbf{x}) = \frac{1}{2}\left(\gamma_x^2 x^2 + \gamma_y^2 y^2 + \gamma_z^2 z^2\right), \text{ with } \gamma_\alpha = \frac{\omega_\alpha}{\omega_m}\ (\alpha = x, y, z).$$

There are two extreme regimes of the interaction parameter β: (1) $\beta = o(1)$, the Eq. (2.4) describes a weakly interacting condensation; (2) $\beta \gg 1$, it corresponds to a strongly interacting condensation or to the semiclassical regime.

There are two typical extreme regimes between the trap frequencies: (1) $\gamma_x = 1$, $\gamma_y \approx 1$ and $\gamma_z \gg 1$, it is a disk-shaped condensation; (2) $\gamma_x \gg 1$, $\gamma_y \gg 1$ and $\gamma_z = 1$, it is a cigar-shaped condensation. In these two cases, the 3-D GPE (2.4) can be approximately reduced to a 2-D and 1-D equation respectively [30, 10, 9] as explained below.

2.2. Reduction to lower dimension. Case I (disk-shaped condensation):

$$\omega_x \approx \omega_y, \quad \omega_z \gg \omega_x, \qquad \Longleftrightarrow \quad \gamma_x = 1,\ \gamma_y \approx 1, \quad \gamma_z \gg 1.$$

Here, the 3-D GPE (2.4) can be reduced to 2-D GPE with $\mathbf{x} = (x, y)$ by assuming that the time evolution does not cause excitations along the z-axis, since the excitations along the z-axis have large energy (of order $\hbar\omega_z$) compared to that along the x and y-axis with energies of order $\hbar\omega_x$. Thus, we may assume that the condensation wave function along the z-axis is always well described by the harmonic oscillator ground state wave function, and set

$$\psi = \psi_2(x, y, t)\phi_{\rm ho}(z) \qquad \text{with} \quad \phi_{\rm ho}(z) = (\gamma_z/\pi)^{1/4}\, e^{-\gamma_z z^2/2}. \tag{2.5}$$

Plugging (2.5) into (2.4), multiplying by $\phi_{\rm ho}^*(z)$ (where f^* denotes the conjugate of a function f), integrating with respect to z over $(-\infty,\infty)$, we get

$$i\,\frac{\partial\psi_2(\mathbf{x},t)}{\partial t} = -\frac{1}{2}\nabla^2\psi_2 + \frac{1}{2}\left(\gamma_x^2x^2+\gamma_y^2y^2+C\right)\psi_2 + \beta_2|\psi_2|^2\psi_2, \tag{2.6}$$

where

$$\beta_2 = \beta\int_{-\infty}^{\infty}\phi_{\rm ho}^4(z)\,dz = \beta\sqrt{\frac{\gamma_z}{2\pi}}, \quad C = \int_{-\infty}^{\infty}\left(\gamma_z^2z^2|\phi_{\rm ho}(z)|^2 + \left|\frac{d\phi_{\rm ho}}{dz}\right|^2\right)\,dz.$$

Since this GPE is time-transverse invariant, we can replace $\psi_2 \to \psi\, e^{-i\frac{Ct}{2}}$ so that the constant C in the trap potential disappears, and we obtain the 2-D effective GPE:

$$i\,\frac{\partial\psi(\mathbf{x},t)}{\partial t} = -\frac{1}{2}\nabla^2\psi + \frac{1}{2}\left(\gamma_x^2x^2+\gamma_y^2y^2\right)\psi + \beta_2|\psi|^2\psi. \tag{2.7}$$

Note that the observables, e.g. the position density $|\psi|^2$, are not affected by dropping the constant C in (2.6).

Case II (cigar-shaped condensation):

$$\omega_x \gg \omega_z, \quad \omega_y \gg \omega_z \qquad \Longleftrightarrow \qquad \gamma_x \gg 1, \quad \gamma_y \gg 1,\ \gamma_z = 1.$$

Here, the 3-D GPE (2.4) can be reduced to a 1-D GPE with $\mathbf{x} = z$. Similarly as in the 2-D case, we can derive the following 1-D GPE [30, 10, 9]:

$$i\,\frac{\partial\psi(z,t)}{\partial t} = -\frac{1}{2}\psi_{zz}(z,t) + \frac{\gamma_z^2z^2}{2}\psi(z,t) + \beta_1|\psi(z,t)|^2\psi(z,t), \tag{2.8}$$

where $\beta_1 = \beta\sqrt{\gamma_x\gamma_y}/2\pi$.

The 3-D GPE (2.4), 2-D GPE (2.7) and 1-D GPE (2.8) can be written in a unified form:

$$i\,\frac{\partial\psi(\mathbf{x},t)}{\partial t} = -\frac{1}{2}\nabla^2\psi + V_d(\mathbf{x})\psi + \beta_d\,|\psi|^2\psi, \quad \mathbf{x}\in\mathbb{R}^d, \tag{2.9}$$

$$\psi(\mathbf{x},0) = \psi_0(\mathbf{x}), \qquad \mathbf{x}\in\mathbb{R}^d, \tag{2.10}$$

with

$$\beta_d = \beta\begin{cases}\sqrt{\gamma_x\gamma_y}/2\pi, \\ \sqrt{\gamma_z/2\pi}, \\ 1,\end{cases} \qquad V_d(\mathbf{x}) = \begin{cases}\gamma_z^2z^2/2, & d=1,\\ \left(\gamma_x^2x^2+\gamma_y^2y^2\right)/2, & d=2,\\ \left(\gamma_x^2x^2+\gamma_y^2y^2+\gamma_z^2z^2\right)/2, & d=3,\end{cases}$$

where $\gamma_x>0$, $\gamma_y>0$ and $\gamma_z>0$ are constants. The normalization condition for (2.9) is

$$N(\psi) = \|\psi(\cdot,t)\|^2 = \int_{\mathbb{R}^d}|\psi(\mathbf{x},t)|^2\,d\mathbf{x} \equiv \int_{\mathbb{R}^d}|\psi_0(\mathbf{x})|^2\,d\mathbf{x} = 1. \tag{2.11}$$

3. Fourth-order time-splitting Laguerre-Hermite pseudospectral method.

In this section we present a fourth-order time-splitting Laguerre-Hermite pseudospectral method for the problem (2.9)-(2.10) in 3-D with cylindrical symmetry. As preparatory steps we begin by introducing the fourth-order time-splitting method

and applying it with Hermite pseudospectral method for 1-D GPE and with Laguerre pseudospectral method for 2-D GPE with radial symmetry, respectively.

Consider a general evolution equation

$$iu_t = f(u) = Au + Bu \tag{3.1}$$

where $f(u)$ is a nonlinear operator and the splitting $f(u) = Au + Bu$ can be quite abitrary, in particular, A and B do not need to commute. For a given time step $\Delta t > 0$, let $t_n = n\ \Delta t$, $n = 0, 1, 2, \ldots$ and u^n be the approximation of $u(t_n)$. A fourth-order symplectic time integrator (cf. [41, 31]) for (3.1) is as follows:

$$\begin{aligned}
u^{(1)} &= e^{-i2w_1 A\Delta t}\ u^n;\\
u^{(2)} &= e^{-i2w_2 B\Delta t}\ u^{(1)};\\
u^{(3)} &= e^{-i2w_3 A\Delta t}\ u^{(2)};\\
u^{(4)} &= e^{-i2w_4 B\Delta t}\ u^{(3)};\\
u^{(5)} &= e^{-i2w_3 A\Delta t}\ u^{(4)};\\
u^{(6)} &= e^{-i2w_2 B\Delta t}\ u^{(5)};\\
u^{n+1} &= e^{-i2w_1 A\Delta t}\ u^{(6)};
\end{aligned} \tag{3.2}$$

where

$$\begin{aligned}
&w_1 = 0.33780\ 17979\ 89914\ 40851,\ w_2 = 0.67560\ 35959\ 79828\ 81702,\\
&w_3 = -0.08780\ 17979\ 89914\ 40851,\ w_4 = -0.85120\ 71979\ 59657\ 63405.
\end{aligned} \tag{3.3}$$

We now rewrite the GPE (2.9) in the form of (3.1) with

$$A\psi = \beta_d\ |\psi(\mathbf{x},t)|^2\psi(\mathbf{x},t), \qquad B\psi = -\frac{1}{2}\nabla^2\psi(\mathbf{x},t) + V_d(\mathbf{x})\psi(\mathbf{x},t). \tag{3.4}$$

Thus, the key for an efficient implementation of (3.2) is to solve efficiently the following two subproblems:

$$i\ \frac{\partial\psi(\mathbf{x},t)}{\partial t} = A\psi(\mathbf{x},t) = \beta_d\ |\psi(\mathbf{x},t)|^2\psi(\mathbf{x},t), \qquad \mathbf{x}\in\mathbb{R}^d, \tag{3.5}$$

and

$$\begin{aligned}
&i\ \frac{\partial\psi(\mathbf{x},t)}{\partial t} = B\psi(\mathbf{x},t) = -\frac{1}{2}\nabla^2\psi(\mathbf{x},t) + V_d(\mathbf{x})\psi(\mathbf{x}), \qquad \mathbf{x}\in\mathbb{R}^d,\\
&\lim_{|\mathbf{x}|\to+\infty}\psi(\mathbf{x},t) = 0.
\end{aligned} \tag{3.6}$$

The decaying condition in (3.6) is necessary for satisfying the normalization (2.11).

Multiplying (3.5) by $\overline{\psi(\mathbf{x},t)}$, we find that the ordinary differential equation (3.5) leaves $|\psi(\mathbf{x},t)|$ invariant in t. Hence, for $t \geq t_s$ (t_s is any given time), (3.5) becomes

$$i\ \frac{\partial\psi(\mathbf{x},t)}{\partial t} = \beta_d\ |\psi(\mathbf{x},t_s)|^2\psi(\mathbf{x},t),\ t\geq t_s, \qquad \mathbf{x}\in\mathbb{R}^d \tag{3.7}$$

which can be integrated **exactly**, i.e.,

$$\psi(\mathbf{x},t) = e^{-i\beta_d|\psi(\mathbf{x},t_s)|^2(t-t_s)}\psi(\mathbf{x},t_s), \qquad t\geq t_s, \quad \mathbf{x}\in\mathbb{R}^d. \tag{3.8}$$

Thus, it remains to find an efficient and accurate scheme for (3.6). We shall construct below suitable spectral basis functions which are eigenfunctions of B so that $e^{-iB\Delta t}\psi$ can be exactly evaluated (which is necessary for the final scheme to be time reversible and time transverse invariant). Hence, the only time discretization error of the corresponding time splitting method (3.2) is the splitting error, which is fourth order in Δt. Furthermore, the scheme is explicit, time reversible and time transverse invariant, and as we shall show below, it is also unconditionally stable.

3.1. Hermite pseudospectral method for the 1-D GPE. In the 1-D case, Eq. (3.6) collapses to

$$i\,\frac{\partial\psi(z,t)}{\partial t} = B\psi(z,t) = -\frac{1}{2}\frac{\partial^2\psi(z,t)}{\partial z^2} + \frac{\gamma_z^2 z^2}{2}\psi(z,t), \quad z\in\mathbb{R}, \tag{3.9}$$

$$\lim_{|z|\to+\infty}\psi(z,t) = 0,\ t\ge 0, \tag{3.10}$$

with the normalization (2.11)

$$\|\psi(\cdot,t)\|^2 = \int_{-\infty}^{\infty}|\psi(z,t)|^2dz \equiv \int_{-\infty}^{\infty}|\psi_0(z)|^2dz = 1. \tag{3.11}$$

Since the above equation is posed on the whole line, it is natural to consider Hermite functions which have been successfully applied to other equations (cf. [22, 27]). Although the standard Hermite functions could be used as basis functions here, they are not the most appropriate. Below, we construct properly scaled Hermite functions which are eigenfunctions of B.

Let $H_l(z)$ $(l = 0, 1, \ldots, N)$ be the standard Hermite polynomials satisfying

$$H_l''(z) - 2zH_l'(z) + 2lH_l(z) = 0, \qquad z\in\mathbb{R}, \quad l\ge 0, \tag{3.12}$$

$$\int_{-\infty}^{\infty} H_l(z)H_n(z)e^{-z^2}\,dz = \sqrt{\pi}\,2^l\,l!\,\delta_{ln}, \qquad l,n\ge 0, \tag{3.13}$$

where δ_{ln} is the Kronecker delta. We define the scaled Hermite function

$$h_l(z) = e^{-\gamma_z z^2/2}\,H_l\left(\sqrt{\gamma_z}z\right)/\sqrt{2^l\,l!}(\pi/\gamma_z)^{1/4}, \qquad z\in\mathbb{R}. \tag{3.14}$$

Plugging (3.14) into (3.12) and (3.13), we find that

$$-\frac{1}{2}h_l''(z) + \frac{\gamma_z^2 z^2}{2}h_l(z) = \mu_l^z h_l(z),\ z\in\mathbb{R}, \qquad \mu_l^z = \frac{2l+1}{2}\gamma_z, \quad l\ge 0, \tag{3.15}$$

$$\int_{-\infty}^{\infty} h_l(z)h_n(z)\,dz = \int_{-\infty}^{\infty}\frac{1}{\sqrt{\pi 2^l l!2^n n!}}H_l(z)H_n(z)e^{-z^2}\,dz = \delta_{ln}, \quad l,n\ge 0. \tag{3.16}$$

Hence, $\{h_l\}$ are eigenfunctions of B defined in (3.9).

For a fixed N, let $X_N = \mathrm{span}\{h_l : l = 0, 1, \cdots, N\}$. The Hermite-spectral method for (3.9) is to find $\psi_N(z,t)\in X_N$, i.e.,

$$\psi_N(z,t) = \sum_{l=0}^{N}\hat{\psi}_l(t)\,h_l(z), \qquad z\in\mathbb{R}. \tag{3.17}$$

such that

$$i\,\frac{\partial\psi_N(z,t)}{\partial t} = B\psi_N(z,t) = -\frac{1}{2}\frac{\partial^2\psi_N(z,t)}{\partial z^2} + \frac{\gamma_z^2 z^2}{2}\psi_N(z,t), \quad z\in\mathbb{R}. \tag{3.18}$$

Note that $\lim_{|z|\to+\infty} h_l(z) = 0$ (cf. [40]) so the decaying condition $\lim_{|z|\to+\infty} \psi_N(z,t) = 0$ is automatically satisfied.

Plugging (3.17) into (3.18), thanks to (3.15) and (3.16), we find

$$i\,\frac{d\hat{\psi}_l(t)}{dt} = \mu_l^z\ \hat{\psi}_l(t) = \frac{2l+1}{2}\gamma_z\ \hat{\psi}_l(t), \qquad l = 0, 1, \cdots, N. \tag{3.19}$$

Hence, the solution for (3.18) is given by

$$\psi_N(z,t) = e^{-iB(t-t_s)}\psi_N(z,t_s) = \sum_{l=0}^{N} e^{-i\mu_l^z\,(t-t_s)}\ \hat{\psi}_l(t_s)h_l(z), \qquad t \geq t_s. \tag{3.20}$$

Let $\{\hat{z}_k\}_{k=0}^N$ be the Hermite-Gauss points (cf. [40, 22]), i.e. $\{\hat{z}_k\}_{k=0}^N$ are the $N+1$ roots of the polynomial $H_{N+1}(z)$. Let ψ_k^n be the approximation of $\psi(z_k,t_n)$ and ψ^n be the solution vector with components ψ_k^n. Then, the fourth-order time-splitting Hermite-pseudospectral (TSHP4) method for 1-D GPE (2.9) is given by

$$\begin{aligned}
\psi_k^{(1)} &= e^{-i2w_1\ \Delta t\ \beta_1|\psi_k^n|^2}\ \psi_k^n,\\
\psi_k^{(2)} &= \sum_{l=0}^{N} e^{-i2w_2\ \mu_l^z\ \Delta t}\ \widehat{(\psi^{(1)})}_l\ h_l(z_k),\\
\psi_k^{(3)} &= e^{-i2w_3\ \Delta t\ \beta_1|\psi_k^{(2)}|^2}\ \psi_k^{(2)},\\
\psi_k^{(4)} &= \sum_{l=0}^{N} e^{-i2w_4\ \mu_l^z\ \Delta t}\ \widehat{(\psi^{(3)})}_l\ h_l(z_k), \qquad k = 0, 1, \ldots, N,\\
\psi_k^{(5)} &= e^{-i2w_3\ \Delta t\ \beta_1|\psi_k^{(4)}|^2}\ \psi_k^{(4)},\\
\psi_k^{(6)} &= \sum_{l=0}^{N} e^{-i2w_2\ \mu_l^z\ \Delta t}\ \widehat{(\psi^{(5)})}_l\ h_l(z_k),\\
\psi_k^{n+1} &= e^{-i2w_1\ \Delta t\ \beta_1|\psi_k^{(6)}|^2}\ \psi_k^{(6)};
\end{aligned} \tag{3.21}$$

where $w_i,\ i = 1, 2, 3, 4$ are given in (3.3), and $\{\widehat{U}_l\}$, the coefficients of scaled Hermite expansion of $U(z)$, can be computed from the discrete scaled Hermite transform:

$$\widehat{U}_l = \sum_{k=0}^{N}\ \omega_k^z\ U(z_k)\ h_l(z_k), \qquad l = 0, 1, \ldots, N. \tag{3.22}$$

In the above, z_k and ω_k^z are the scaled Hermite-Gauss points and weights, respectively, which are defined by

$$\omega_k^z = \frac{\hat{\omega}_k^z\ e^{\hat{z}_k^2}}{\sqrt{\gamma_z}}, \qquad z_k = \frac{\hat{z}_k}{\sqrt{\gamma_z}}, \qquad 0 \leq k \leq N, \tag{3.23}$$

where $\{\hat{\omega}_k^z\}_{k=0}^N$ are the weights associated with the Hermite-Gauss quadrature (cf. [22]) satisfying

$$\sum_{k=0}^{N}\ \hat{\omega}_k^z\ \frac{H_l(\hat{z}_k)}{\pi^{1/4}\sqrt{2^l\,l!}}\ \frac{H_n(\hat{z}_k)}{\pi^{1/4}\sqrt{2^n\,n!}} = \delta_{ln}, \qquad l, n = 0, 1, \ldots, N, \tag{3.24}$$

and we derive from (3.14) that

$$\sum_{k=0}^{N} \omega_k^z \, h_l(z_k) \, h_m(z_k) = \sum_{k=0}^{N} \hat{\omega}_k^z \, e^{\hat{z}_k^2}/\sqrt{\gamma_z} \, h_l\left(\hat{z}_k/\sqrt{\gamma_z}\right) \, h_m\left(\hat{z}_k/\sqrt{\gamma_z}\right)$$
$$= \sum_{k=0}^{N} \hat{\omega}_k^z \, \frac{H_l(\hat{z}_k)}{\pi^{1/4}\sqrt{2^l \, l!}} \, \frac{H_n(\hat{z}_k)}{\pi^{1/4}\sqrt{2^n \, n!}} = \delta_{ln}, \; 0 \le l, n \le N. \quad (3.25)$$

Note that the computation of $\{\omega_k^z\}$ from (3.23) is not a stable process for very large N. However, one can compute $\{\omega_k^z\}$ in a stable way as suggested in the Appendix of [38].

Thus, the memory requirement of this scheme is $O(N)$ and the computational cost per time step is a small multiple of N^2. As for the stability of the TSHP4, we have the following

LEMMA 3.1. *The time-splitting Hermite-pseudospectral (TSHP4) method (3.21) is unconditionally stable. More precisely, we have*

$$\|\psi^n\|_{l^2}^2 = \sum_{k=0}^{N} \omega_k^z |\psi_k^n|^2 = \sum_{k=0}^{M} \omega_k^z |\psi_0(z_k)|^2 = \|\psi_0\|_{l^2}^2, \qquad n = 0, 1, \ldots . \quad (3.26)$$

Proof. From (3.21), noting (3.22) and (3.25), we obtain

$$\|\psi^{n+1}\|_{l^2}^2 = \sum_{k=0}^{N} \omega_k^z |\psi_k^n|^2 = \sum_{k=0}^{N} \omega_k^z \left| e^{-i2w_1 \, \Delta t \, \beta_1 |\psi_k^{(6)}|^2} \, \psi_k^{(6)} \right|^2$$
$$= \sum_{k=0}^{N} \omega_k^z |\psi_k^{(6)}|^2 = \sum_{k=0}^{N} \omega_k^z \left| \sum_{l=0}^{N} e^{-i2w_2 \, \mu_l^z \, \Delta t} \, \widehat{(\psi^{(5)})}_l \, h_l(z_k) \right|^2$$
$$= \sum_{l=0}^{N} \sum_{m=0}^{N} e^{-i2w_2 \, \mu_l^z \, \Delta t} \, \widehat{(\psi^{(5)})}_l e^{i2w_2 \, \mu_m^z \, \Delta t} \, (\widehat{(\psi^{(5)})}_m)^* \left[\sum_{k=0}^{N} \omega_k^z h_l(z_k) h_m(z_k) \right]$$
$$= \sum_{l=0}^{N} \sum_{m=0}^{N} e^{-i2w_2 \, \mu_l^z \, \Delta t} \, \widehat{(\psi^{(5)})}_l e^{i2w_2 \, \mu_m^z \, \Delta t} \, (\widehat{(\psi^{(5)})}_m)^* \, \delta_{lm}$$
$$= \sum_{l=0}^{N} |\widehat{(\psi^{(5)})}_l|^2 = \sum_{l=0}^{N} \left| \sum_{k=0}^{N} \omega_k^z \, \psi^{(5)}(z_k) \, h_l(z_k) \right|^2$$
$$= \sum_{k=0}^{N} \sum_{m=0}^{N} \omega_k^z \psi^{(5)}(z_k) \psi^{(5)}(z_m)^* \left[\sum_{l=0}^{N} \omega_m^z h_l(z_k) h_l(z_m) \right]$$
$$= \sum_{k=0}^{N} \sum_{m=0}^{N} \omega_k^z \psi^{(5)}(z_k) \psi^{(5)}(z_m)^* \, \delta_{km}$$
$$= \sum_{k=0}^{N} \omega_k^z |\psi^{(5)}(z_k)|^2 = \|\psi^{(5)}\|_{l^2}^2. \quad (3.27)$$

Similarly, we have

$$\|\psi^{n+1}\|_{l^2}^2 = \|\psi^{(5)}\|_{l^2}^2 = \|\psi^{(3)}\|_{l^2}^2 = \|\psi^{(1)}\|_{l^2}^2 = \|\psi^n\|_{l^2}^2, \qquad n \ge 0. \quad (3.28)$$

Thus the equality (3.26) can be obtained from (3.28) by induction. □

REMARK 3.1. *Extension of TSHP4 method (3.21) to 2-D GPE without radial symmetry and 3-D GPE without cylindrical symmetry is straightforward by using tensor product of scaled Hermite functions.*

3.2. Laguerre pseudospectral method for 2-D GPE with radial symmetry. In the 2-D case with radial symmetry, i.e. $d = 2$ and $\gamma_x = \gamma_y$ in (2.9), and $\psi_0(x, y) = \psi_0(r)$ in (2.10) with $r = \sqrt{x^2 + y^2}$, we can write the solution of (2.9), (2.10) as $\psi(x, y, t) = \psi(r, t)$. Therefore, Eq. (3.6) collapses to

$$i\,\frac{\partial\psi(r,t)}{\partial t} = B\psi(r,t) = -\frac{1}{2r}\frac{\partial}{\partial r}\left(r\frac{\partial\psi(r,t)}{\partial r}\right) + \frac{\gamma_r^2 r^2}{2}\psi(r,t), \quad 0 < r < \infty, \tag{3.29}$$

$$\lim_{r\to\infty}\psi(r,t) = 0, \qquad t \geq 0, \tag{3.30}$$

where $\gamma_r = \gamma_x = \gamma_y$. The normalization (2.11) collapses to

$$\|\psi(\cdot,t)\|^2 = 2\pi\int_0^\infty |\psi(r,t)|^2 r\,dr \equiv 2\pi\int_0^\infty |\psi_0(r)|^2 r\,dr = 1. \tag{3.31}$$

Note that it can be shown, similarly as for the Poisson equation in a 2-D disk (cf. [37]), that the problem (3.29)-(3.30) admits a unique solution without any condition at the pole $r = 0$.

Since (3.29) is posed on a semi-infinite interval, it is natural to consider Laguerre functions which have been successfully used for other problems in semi-infinite intervals (cf. [22, 38]). Again, the standard Laguerre functions, although usable, are not the most appropriate for this problem. Below, we construct properly scaled Laguerre functions which are eigenfunctions of B.

Let $\hat{L}_m(r)$ $(m = 0, 1, \ldots, M)$ be the Laguerre polynomials of degree m satisfying

$$r\hat{L}_m''(r) + (1-r)\hat{L}_m'(r) + m\hat{L}_m(r) = 0, \qquad m = 0, 1, \ldots, \tag{3.32}$$

$$\int_0^\infty e^{-r}\,\hat{L}_m(r)\,\hat{L}_n(r)\,dr = \delta_{mn}, \qquad m, n = 0, 1, \ldots\,. \tag{3.33}$$

We define the scaled Laguerre functions L_m by

$$L_m(r) = \sqrt{\frac{\gamma_r}{\pi}}\;e^{-\gamma_r r^2/2}\;\hat{L}_m(\gamma_r r^2), \qquad 0 \leq r < \infty. \tag{3.34}$$

Note that $\lim_{|r|\to+\infty} L_m(r) = 0$ (cf. [40]) hence, $\lim_{|r|\to+\infty}\psi_M(r,t) = 0$ is automatically satisfied.

Plugging (3.34) into (3.32) and (3.33), a simple computation shows

$$-\frac{1}{2r}\frac{\partial}{\partial r}\left(r\frac{\partial L_m(r)}{\partial r}\right) + \frac{1}{2}\gamma_r^2 r^2 L_m(r) = \mu_m^r L_m(r),\ \mu_m^r = \gamma_r(2m+1),\ m \geq 0, \tag{3.35}$$

$$2\pi\int_0^\infty L_m(r)L_n(r)r\,dr = \int_0^\infty e^{-r}\hat{L}_m(r)\hat{L}_n(r)\,dr = \delta_{mn}, \quad m, n \geq 0. \tag{3.36}$$

Hence, $\{L_m\}$ are eigenfunctions of B defined in (3.29).

For a fixed M, let $Y_M = \text{span}\{L_m : m = 0, 1, \cdots, M\}$. The Laguerre-spectral method for (3.9) is to find $\psi_M(r,t) \in Y_M$, i.e.,

$$\psi_M(r,t) = \sum_{m=0}^{M}\hat{\psi}_m(t)\,L_m(r), \qquad 0 \leq r < \infty \tag{3.37}$$

such that

$$i\,\frac{\partial\psi_M(r,t)}{\partial t} = B\psi_M(r,t) = -\frac{1}{2r}\frac{\partial}{\partial r}\left(r\frac{\partial\psi_M(r,t)}{\partial r}\right) + \frac{\gamma_r^2 r^2}{2}\psi_M(r,t), \quad 0 < r < \infty. \tag{3.38}$$

Plugging (3.37) into (3.38), thanks to (3.35) and (3.36), we find

$$i\,\frac{d\hat{\psi}_m(t)}{dt} = \mu_m^r\hat{\psi}_m(t) = \gamma_z(2m+1)\hat{\psi}_m(t),\ m = 0, 1, \cdots, M. \tag{3.39}$$

Hence, the solution for (3.38) is given by

$$\psi_M(r,t) = e^{-iB(t-t_s)}\psi_M(r,t_s) = \sum_{m=0}^{M} e^{-i\mu_m^r(t-t_s)}\ \hat{\psi}_m(t_s)L_m(r), \qquad t \geq t_s. \tag{3.40}$$

Let $\{\hat{r}_j\}_{j=0}^M$ be the Laguerre-Gauss-Radau points (cf. [22]), i.e. they are the $M+1$ roots of the polynomial $r\hat{L}'_{M+1}(r)$. Let ψ_j^n be the approximation of $\psi(r_j, t_n)$ and ψ^n be the solution vector with components ψ_j^n. Then, the fourth-order time-splitting Laguerre-pseudospectral (TSLP4) method for 2-D GPE (2.9) with radial symmetry is given by

$$\begin{aligned}
\psi_j^{(1)} &= e^{-i2w_1\ \Delta t\ \beta_2|\psi_j^n|^2}\ \psi_j^n,\\
\psi_j^{(2)} &= \sum_{l=0}^{M} e^{-i2w_2\ \mu_l^r\ \Delta t}\ \widehat{(\psi^{(1)})}_l\ L_l(r_j),\\
\psi_j^{(3)} &= e^{-i2w_3\ \Delta t\ \beta_2|\psi_j^{(2)}|^2}\ \psi_j^{(2)},\\
\psi_j^{(4)} &= \sum_{l=0}^{M} e^{-i2w_4\ \mu_l^r\ \Delta t}\ \widehat{(\psi^{(3)})}_l\ L_l(r_j), \qquad j = 0, 1, \ldots, M,\\
\psi_j^{(5)} &= e^{-i2w_3\ \Delta t\ \beta_2|\psi_j^{(4)}|^2}\ \psi_j^{(4)},\\
\psi_j^{(6)} &= \sum_{l=0}^{M} e^{-i2w_2\ \mu_l^r\ \Delta t}\ \widehat{(\psi^{(5)})}_l\ L_l(r_j),\\
\psi_j^{n+1} &= e^{-i2w_1\ \Delta t\ \beta_2|\psi_j^{(6)}|^2}\ \psi_j^{(6)};
\end{aligned} \tag{3.41}$$

where $\widehat{U}_l$, the coefficients of scaled Laguerre expansion of $U(r)$ can be computed from the discrete scaled Laguerre transform:

$$\widehat{U}_l = \sum_{j=0}^{M} \omega_j^r\ U(r_j)\ L_l(r_j), \qquad l = 0, 1, \ldots, M. \tag{3.42}$$

In the above, r_j and ω_j^z are the scaled Laguerre-Gauss-Radau points and weights, respectively, which are defined by

$$\omega_j^r = \frac{\pi}{\gamma_r}\ \hat{\omega}_j^r\ e^{\hat{r}_j}, \qquad r_j = \sqrt{\frac{\hat{r}_j}{\gamma_r}}, \qquad j = 0, 1, \ldots, M, \tag{3.43}$$

where $\{\hat{\omega}_j^r\}_{j=0}^M$ are the weights associated to the Laguerre-Gauss quadrature [22] satisfying

$$\sum_{j=0}^{M} \hat{\omega}_j^r \hat{L}_m(\hat{r}_j)\hat{L}_n(\hat{r}_j) = \delta_{nm}, \qquad n, m = 0, 1, \ldots, M,$$

and we derive from (3.34) that

$$\sum_{j=0}^{M} \omega_j^r L_m(r_j) L_n(r_j) = \sum_{j=0}^{M} \hat{\omega}_j^r e^{\hat{r}_j} \pi/\gamma_r \; L_m\left(\sqrt{\hat{r}_j/\gamma_r}\right) \; L_n\left(\sqrt{\hat{r}_j/\gamma_r}\right)$$
$$= \sum_{j=0}^{M} \hat{\omega}_j^r \hat{L}_m(\hat{r}_j)\hat{L}_n(\hat{r}_j) = \delta_{nm}, \quad n,m = 0,1,\ldots,M. \tag{3.44}$$

As in the Hermite case, the computation of $\{\omega_j^r\}$ from (3.43) is not a stable process for very large N. However, one can compute $\{\omega_j^r\}$ in a stable way as suggested in the Appendix of [38].

The memory requirement of this scheme is $O(M)$ and the computational cost per time step is a small multiple of M^2. As for the stability of the TSLP4, we have the following

LEMMA 3.2. *The time-splitting Laguerre-pseudospectral (TSLP4) method (3.41) is unconditionally stable. More precisely, we have*

$$\|\psi^n\|_{l^2}^2 = \sum_{j=0}^{M} \omega_j^r |\psi_j^n|^2 = \sum_{j=0}^{M} \omega_j^r |\psi_0(r_j)|^2 = \|\psi_0\|_{l^2}^2, \qquad n \geq 0.$$

Proof. Using (3.44), the proof is essentially the same as in Lemma 3.1 for time-splitting Hermite-pseudospectral method. □

3.3. Laguerre-Hermite pseudospectral method for 3-D GPE with cylindrical symmetry. In the 3-D case with cylindrical symmetry, i.e. $d = 3$ and $\gamma_x = \gamma_y$ in (2.9), and $\psi_0(x,y,z) = \psi_0(r,z)$ in (2.10), the solution of (2.9)-(2.10) with $d = 3$ satisfies $\psi(x,y,z,t) = \psi(r,z,t)$. Therefore, Eq. (3.6) becomes to

$$i\,\frac{\partial \psi(r,z,t)}{\partial t} = B\psi(r,z,t) = -\frac{1}{2}\left[\frac{1}{r}\frac{\partial}{\partial r}\left(r\frac{\partial \psi}{\partial r}\right) + \frac{\partial^2 \psi}{\partial z^2}\right] + \frac{1}{2}\left(\gamma_r^2 r^2 + \gamma_z^2 z^2\right)\psi,$$
$$0 < r < \infty, \; -\infty < z < \infty, \tag{3.45}$$
$$\lim_{r\to\infty} \psi(r,z,t) = 0, \quad \lim_{|z|\to\infty} \psi(r,z,t) = 0, \qquad t \geq 0, \tag{3.46}$$

where $\gamma_r = \gamma_x = \gamma_y$. The normalization (2.11) becomes

$$\|\psi(\cdot,t)\|^2 = 2\pi \int_0^\infty \int_{-\infty}^\infty |\psi(r,z,t)|^2 r \; drdz \equiv 2\pi \int_0^\infty \int_{-\infty}^\infty |\psi_0(r,z)|^2 r \; drdz = 1. \tag{3.47}$$

We are now in position to present our Laguerre-Hermite pseudospectral method for (3.45).

Using the same notations as in previous subsections, we derive from (3.15) and (3.35) that

$$-\frac{1}{2}\left[\frac{1}{r}\frac{\partial}{\partial r}\left(r\frac{\partial}{\partial r}\right) + \frac{\partial^2}{\partial z^2}\right](L_m(r)\; h_l(z)) + \frac{1}{2}\left(\gamma_r^2 r^2 + \gamma_z^2 z^2\right)(L_m(r)\; h_l(z))$$
$$= \left[-\frac{1}{2r}\frac{d}{dr}\left(r\frac{dL_m(r)}{dr}\right) + \frac{1}{2}\gamma_r^2 r^2 L_m(r)\right] h_l(z) + \left[-\frac{1}{2}\frac{d^2 h_l(z)}{dz^2} + \frac{1}{2}\gamma_z^2 z^2 h_l(z)\right] L_m(r)$$
$$= \mu_m^r L_m(r) h_l(z) + \mu_l^z h_l(z) L_m(r) = (\mu_m^r + \mu_l^z) L_m(r) h_l(z). \tag{3.48}$$

Hence, $\{L_m(r)h_l(z)\}$ are eigenfunctions of B defined in (3.45).

For a fixed pair (M,N), let $X_{MN} = \text{span}\{L_m(r)h_l(z) : m = 0,1,\cdots,M,\ l = 0,1,\cdots,N\}$. The Laguerre-Hermite spectral method for (3.45) is to find $\psi_{MN}(r,z,t) \in X_{MN}$, i.e.,

$$\psi_{MN}(r,z,t) = \sum_{m=0}^{M}\sum_{l=0}^{N} \tilde{\psi}_{ml}(t)\ L_m(r)\ h_l(z) \tag{3.49}$$

such that

$$\begin{aligned} i\ \frac{\partial \psi_{MN}(r,z,t)}{\partial t} &= B\psi_{MN}(r,z,t) \\ &= -\frac{1}{2}\left[\frac{1}{r}\frac{\partial}{\partial r}\left(r\frac{\partial \psi_{MN}}{\partial r}\right) + \frac{\partial^2 \psi_{MN}}{\partial z^2}\right] + \frac{1}{2}\left(\gamma_r^2 r^2 + \gamma_z^2 z^2\right)\psi_{MN}. \end{aligned} \tag{3.50}$$

Plugging (3.49) into (3.50), thanks to (3.48), we find that

$$i\ \frac{d\tilde{\psi}_{ml}(t)}{dt} = (\mu_m^r + \mu_l^z)\,\tilde{\psi}_{ml}(t),\ m = 0,1,\cdots,M,\ l = 0,1,\cdots,N. \tag{3.51}$$

Hence, the solution for (3.50) is given by

$$\begin{aligned} \psi_{MN}(r,z,t) &= e^{-iB(t-t_s)}\psi_{MN}(r,z,t_s) \\ &= \sum_{m=0}^{M}\sum_{l=0}^{N} e^{-i(\mu_m^r+\mu_l^z)(t-t_s)}\tilde{\psi}_{ml}(t_s)L_m(r)\ h_l(z), \qquad t \ge t_s. \end{aligned} \tag{3.52}$$

Let ψ_{jk}^n be the approximation of $\psi(r_j,z_k,t_n)$ and ψ^n be the solution vector with components ψ_{jk}^n. The fourth-order time-splitting Laguerre-Hermite-pseudospectral (TSLHP4) method for 3-D GPE (2.9) with cylindrical symmetry is given by

$$\begin{aligned} \psi_{jk}^{(1)} &= e^{-i2w_1\ \Delta t\ \beta_3|\psi_{jk}^n|^2}\ \psi_{jk}^n, \\ \psi_{jk}^{(2)} &= \sum_{m=0}^{M}\sum_{l=0}^{N} e^{-i2w_2\Delta t(\mu_m^r+\mu_l^z)}\ \widehat{(\psi^{(1)})}_{ml}\ L_m(r_j)h_l(z_k), \\ \psi_{jk}^{(3)} &= e^{-i2w_3\ \Delta t\ \beta_3|\psi_{jk}^{(2)}|^2}\ \psi_{jk}^{(2)}, \\ \psi_{jk}^{(4)} &= \sum_{m=0}^{M}\sum_{l=0}^{N} e^{-i2w_4\Delta t(\mu_m^r+\mu_l^z)}\ \widehat{(\psi^{(3)})}_{ml}\ L_m(r_j)h_l(z_k), \\ \psi_{jk}^{(5)} &= e^{-i2w_3\ \Delta t\ \beta_3|\psi_{jk}^{(4)}|^2}\ \psi_{jk}^{(4)}, \quad j = 0,1,\ldots,M,\ k = 0,1\ldots,N, \\ \psi_{jk}^{(6)} &= \sum_{m=0}^{M}\sum_{l=0}^{N} e^{-i2w_2\Delta t(\mu_m^r+\mu_l^z)}\ \widehat{(\psi^{(5)})}_{ml}\ L_m(r_j)h_l(z_k), \\ \psi_{jk}^{n+1} &= e^{-i2w_1\ \Delta t\ \beta_3|\psi_{jk}^{(6)}|^2}\ \psi_{jk}^{(6)}; \end{aligned} \tag{3.53}$$

where $\widehat{U}_{ml}$, the coefficients of scaled Laguerre-Hermite expansion of $U(r,z)$ are computed by the discrete scaled Laguerre-Hermite transform

$$\widehat{U}_{ml} = \sum_{j=0}^{M}\sum_{k=0}^{N} \omega_j^r\ \omega_k^z\ U(r_j,z_k)\ L_m(r_j)h_l(z_k),\ m = 0,1,\ldots,M,\ k = 0,1,\ldots,N. \tag{3.54}$$

The memory requirement of this scheme is $O(MN)$ and the computational cost per time step is $O(\max(M^2N, N^2M))$. As for the stability of the TSLHP4, we have the following

LEMMA 3.3. *The time-splitting Laguerre-Hermite pseudospectral (TSLHP4) method (3.53) is unconditionally stable. More precisely, we have*

$$\|\psi^n\|_{l^2}^2 = \sum_{j=0}^{M}\sum_{k=0}^{N} \omega_j^r \omega_k^z |\psi_{jk}^n|^2 = \sum_{j=0}^{M}\sum_{k=0}^{N} \omega_j^r \omega_k^z |\psi_0(r_j, z_k)|^2 = \|\psi_0\|_{l^2}^2, \quad n \geq 0.$$

Proof. Using (3.25) and (3.44), the proof is essentially the same as in Lemma 3.1 for time-splitting Hermite-pseudospectral method. □

4. Extension to multi-component BECs. The time-splitting Laguerre-Hermite pseudospectral method, introduced above for the 3-D GPE with cylindrical symmetry, can be extended to vector Gross-Pitaevskii equations (VGPEs) for multi-component BECs [5]. For simplicity, we only present the detailed method for the dynamics of two-component BECs. Consider the dimensionless VGPEs with an external driven filed (cf. [5])

$$i\,\frac{\partial\psi(r,z,t)}{\partial t} = -\frac{1}{2}\left[\frac{1}{r}\frac{\partial}{\partial r}\left(r\frac{\partial\psi}{\partial r}\right) + \frac{\partial^2\psi}{\partial z^2}\right] + \frac{1}{2}\left(\gamma_r^2 r^2 + \gamma_z^2 (z - z_1^0)^2\right)\psi \tag{4.1}$$
$$+ \left(\beta_{11}|\psi|^2 + \beta_{12}|\phi|^2\right)\psi + \sqrt{N_2^0/N_1^0}\, f(t)\phi,$$
$$i\,\frac{\partial\phi(r,z,t)}{\partial t} = -\frac{1}{2}\left[\frac{1}{r}\frac{\partial}{\partial r}\left(r\frac{\partial\phi}{\partial r}\right) + \frac{\partial^2\phi}{\partial z^2}\right] + \frac{1}{2}\left(\gamma_r^2 r^2 + \gamma_z^2 (z - z_2^0)^2\right)\phi \tag{4.2}$$
$$+ \left(\beta_{21}|\psi|^2 + \beta_{22}|\phi|^2\right)\phi + \sqrt{N_1^0/N_2^0}\, f(t)\psi,\ 0 < r < \infty,\ z \in \mathbb{R},$$
$$\lim_{r\to\infty}\psi(r,z,t) = \lim_{r\to\infty}\phi(r,z,t) = 0, \quad \lim_{|z|\to\infty}\psi(r,z,t) = \lim_{|z|\to\infty}\phi(r,z,t) = 0, \tag{4.3}$$
$$\psi(r,z,0) = \psi_0(r,z), \qquad \phi(r,z,0) = \phi_0(r,z); \tag{4.4}$$

where z_j^0 and N_j^0 $(j = 1, 2)$ are the center of trapping potential along z-axis and the number of atoms of the jth component, respectively; $\gamma_r = \omega_r/\omega_m$, $\gamma_z = \omega_z/\omega_m$ with ω_r, ω_z and ω_m are the radial, axial and reference frequencies, respectively; $\beta_{jl} = 4\pi a_{jl} N_l^0/a_0$ $(j, l = 1, 2)$ with the s-wave scattering length $a_{jl} = a_{lj}$ between the jth and lth component and $a_0 = \sqrt{\hbar/m\omega_m}$; and $f(t) = \Omega\cos(\omega_d t/\omega_m)/\omega_m$ with Ω and ω_d being the amplitude and frequency of the external driven field. The wave functions are normalized as

$$\|\psi_0\|^2 = 2\pi\int_0^\infty\int_{-\infty}^\infty |\psi_0(r,z)|^2 r\, drdz = 1,$$
$$\|\phi_0\|^2 = 2\pi\int_0^\infty\int_{-\infty}^\infty |\phi_0(r,z)|^2 r\, drdz = 1. \tag{4.5}$$

It is easy to show (cf. [5]) that the total number of atoms is conserved

$$N_1^0\|\psi(\cdot,t)\|^2 + N_2^0\|\phi(\cdot,t)\|^2 = 2\pi\int_0^\infty\int_{-\infty}^\infty \left(|\psi(r,z,t)|^2 + |\phi(r,z,t)|^2\right) r\, drdz$$
$$\equiv N_1^0\|\psi_0\|^2 + N_2^0\|\phi_0\|^2 = N_1^0 + N_2^0. \tag{4.6}$$

Unlike the time-splitting Laguerre-Hermite method for 3-D GPE (2.9) with cylindrical symmetry, here we have to split the VGPEs (4.1)-(4.2) into three sub-systems. For example, for a fist-order splitting scheme, we first solve

$$i\,\frac{\partial\psi(r,z,t)}{\partial t} = -\frac{1}{2}\left[\frac{1}{r}\frac{\partial}{\partial r}\left(r\frac{\partial\psi}{\partial r}\right)+\frac{\partial^2\psi}{\partial z^2}\right]+\frac{1}{2}\left(\gamma_r^2r^2+\gamma_z^2z^2\right)\psi, \tag{4.7}$$

$$i\,\frac{\partial\phi(r,z,t)}{\partial t} = -\frac{1}{2}\left[\frac{1}{r}\frac{\partial}{\partial r}\left(r\frac{\partial\phi}{\partial r}\right)+\frac{\partial^2\phi}{\partial z^2}\right]+\frac{1}{2}\left(\gamma_r^2r^2+\gamma_z^2z^2\right)\phi, \tag{4.8}$$

for the time step of length Δt, followed by solving

$$i\,\frac{\partial\psi(r,z,t)}{\partial t} = \frac{1}{2}\gamma_z^2z_1^0(z_1^0-2z)\psi+\left(\beta_{11}|\psi|^2+\beta_{12}|\phi|^2\right)\psi, \tag{4.9}$$

$$i\,\frac{\partial\phi(r,z,t)}{\partial t} = \frac{1}{2}\gamma_z^2z_2^0(z_2^0-2z)\phi+\left(\beta_{21}|\psi|^2+\beta_{22}|\phi|^2\right)\phi, \tag{4.10}$$

for the same time step, and then by solving

$$i\,\frac{\partial\psi(r,z,t)}{\partial t} = \sqrt{N_2^0/N_1^0}\,f(t)\,\phi, \tag{4.11}$$

$$i\,\frac{\partial\phi(r,z,t)}{\partial t} = \sqrt{N_1^0/N_2^0}\,f(t)\,\psi, \tag{4.12}$$

for the same time step.

The nonlinear ODE system (4.9)-(4.10) leaves $|\psi(r,z,t)|$ and $|\phi(r,z,t)|$ invariant in t and thus can be integrated **exactly** [5]. The linear ODE system (4.11)-(4.12) can also be integrated **exactly** by applying a matrix diagonalization technique (cf. [5]). As is shown above, (4.7)-(4.8) can be discretized in space by Laguerre-Hermite pseudospectral method and integrated in time **exactly**.

Let ψ_{jk}^n and ϕ_{jk}^n be the approximations of $\psi(r_j,z_k,t_n)$ and $\phi(r_j,z_k,t_n)$, respectively, and ψ^n and ϕ^n be the solution vectors with components ψ_{jk}^n and ϕ_{jk}^n, respectively. Although it is not clear how to construct a fourth-order time splitting schemes with three sub-systems, a second-order scheme can be easily constructed using the Strang splitting (cf. [39]). More precisely, from time $t=t_n$ to $t=t_{n+1}$, we proceed

as follows:

$$
\begin{aligned}
\psi_{jk}^{(1)} &= \sum_{m=0}^{M}\sum_{l=0}^{N} e^{-i(\mu_m^r+\mu_l^z)\Delta t/2}\ \widehat{(\psi^{(1)})}_{ml}\ L_m(r_j)h_l(z_k),\\
\phi_{jk}^{(1)} &= \sum_{m=0}^{M}\sum_{l=0}^{N} e^{-i(\mu_m^r+\mu_l^z)\Delta t/2}\ \widehat{(\phi^{(1)})}_{ml}\ L_m(r_j)h_l(z_k),\\
\psi_{jk}^{(2)} &= e^{-i[\gamma_z^2 z_1^0(z_1^0-2z_k)/2+(\beta_{11}|\psi_{jk}^{(1)}|^2+\beta_{12}|\phi_{jk}^{(1)}|^2)]\Delta t/2}\psi_{jk}^{(1)},\\
\phi_{jk}^{(2)} &= e^{-i[\gamma_z^2 z_2^0(z_2^0-2z_k)/2+(\beta_{21}|\psi_{jk}^{(1)}|^2+\beta_{22}|\phi_{jk}^{(1)}|^2)]\Delta t/2}\phi_{jk}^{(1)},\\
\psi_{jk}^{(3)} &= \cos(g(t_{n+1},t_n))\psi_{jk}^{(2)} - i\sin(g(t_{n+1},t_n))\sqrt{N_2^0/N_1^0}\phi_{jk}^{(2)},\\
\phi_{jk}^{(3)} &= -i\sin(g(t_{n+1},t_n))\sqrt{N_1^0/N_2^0}\psi_{jk}^{(2)} + \cos(g(t_{n+1},t_n))\phi_{jk}^{(2)},\\
\psi_{jk}^{(4)} &= e^{-i[\gamma_z^2 z_1^0(z_1^0-2)/2+(\beta_{11}|\psi_{jk}^{(3)}|^2+\beta_{12}|\phi_{jk}^{(3)}|^2)]\Delta t/2}\psi_{jk}^{(3)},\\
\phi_{jk}^{(4)} &= e^{-i[\gamma_z^2 z_2^0(z_2^0-2)/2+(\beta_{21}|\psi_{jk}^{(3)}|^2+\beta_{22}|\phi_{jk}^{(3)}|^2)]\Delta t/2}\phi_{jk}^{(3)}, \quad 0\le j\le M,\ 0\le k\le N,\\
\psi_{jk}^{n+1} &= \sum_{m=0}^{M}\sum_{l=0}^{N} e^{-i(\mu_m^r+\mu_l^z)\Delta t/2}\ \widehat{(\psi^{(4)})}_{ml}\ L_m(r_j)h_l(z_k),\\
\phi_{jk}^{n+1} &= \sum_{m=0}^{M}\sum_{l=0}^{N} e^{-i(\mu_m^r+\mu_l^z)\Delta t/2}\ \widehat{(\phi^{(4)})}_{ml}\ L_m(r_j)h_l(z_k),
\end{aligned}
\tag{4.13}
$$

where

$$
g(t,t_n) = \int_{t_n}^{t} f(s)\,ds = \Omega\omega_d\left[\sin(\omega_d t/\omega_m) - \sin(\omega_d t_n/\omega_m)\right].
$$

Note that the only time discretization error of this scheme is the splitting error, which is of second order in Δt. The scheme is explicit, spectral accurate in space and second order accurate in time. The memory requirement of this method is $O(MN)$ and the computational cost per time step is $O(\max(M^2N, MN^2))$. As for the stability, we can prove as in [5] the following lemma, which shows that the total number of atoms is conserved in the discretized level.

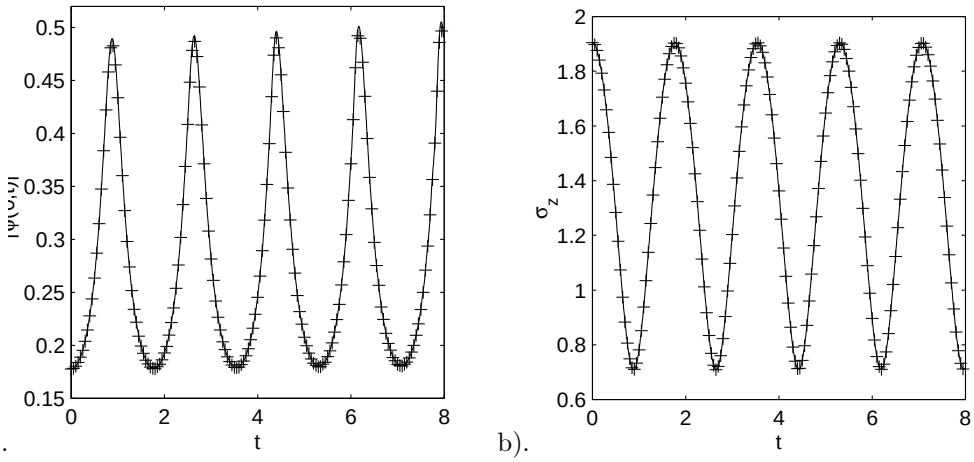
LEMMA 4.1. *The time-splitting Laguerre-Hermite-pseudospectral method (4.13) for multi-component BEC is unconditionally stable. More precisely, we have*

$$
N_1^0\|\psi^n\|_{l^2}^2 + N_2^0\|\phi^n\|_{l^2}^2 = N_1^0\|\psi_0\|_{l^2}^2 + N_2^0\|\phi_0\|_{l^2}^2, \quad n\ge 0.
$$

5. Numerical results. We now present some numerical results by using the numerical methods introduced in section 3. To quantify the numerical results, we define the condensate width along r- and z-axis as

$$
\sigma_\alpha^2 = \int_{\mathbb{R}^d} \alpha^2|\psi(\mathbf{x},t)|\,d\mathbf{x}, \quad \alpha = x,y,z, \qquad \sigma_r^2 = \sigma_x^2 + \sigma_y^2.
$$

Example 1. The 1-D Gross-Pitaevskii equation: We choose $d = 1$, $\gamma_z = 2$, $\beta_1 = 50$ in (2.9). The initial data $\psi_0(z)$ is chosen as the ground state of the 1-D GPE (2.9) with $d = 1$, $\gamma_z = 1$ and $\beta_1 = 50$ [6, 9]. This corresponds to an experimental



a). b).

Figure 1: Evolution of central density and condensate width in Example 1. '—': 'exact solutions' obtained by TSSP [10] with 1025 grid points over an interval $[-12, 12]$; '+ + + ': Numerical results by TSHP4 (3.21) with 31 grid points on the whole z-axis. a). Central density $|\psi(0,t)|^2$; b). condensate width σ_z.

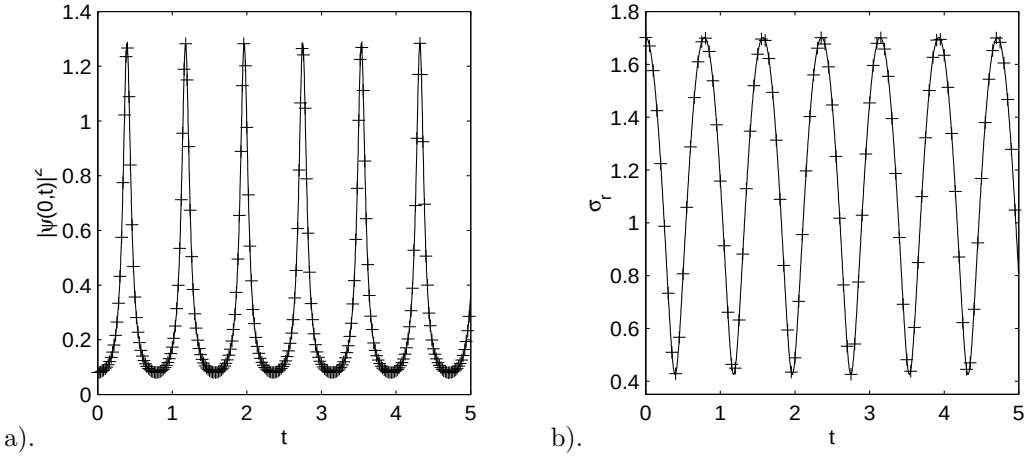
setup where initially the condensate is assumed to be in its ground state, and the trap frequency is double at $t = 0$. We solve this problem by using (3.21) with $N = 31$ and time step $k = 0.001$. Figure 1 plots the condensate width and central density $|\psi(0,t)|^2$ as functions of time. Our numerical experiments also show that the scheme (3.21) with $N = 31$ gives similar numerical results as the TSSP method [10, 11] for this example with 129 grid points over the interval $[-12, 12]$ and time step $k = 0.001$.

Example 2. The 2-D Gross-Pitaevskii equation with radial symmetry: we choose $d = 2$, $\gamma_r = \gamma_x = \gamma_y = 2$, $\beta_2 = 50$ in (2.9). The initial data $\psi_0(r)$ is chosen as the ground state of the 2-D GPE (2.9) with $d = 2$, $\gamma_r = \gamma_x = \gamma_y = 1$ and $\beta_2 = 50$ [6, 9]. Again this corresponds to an experimental setup where initially the condensate is assumed to be in its ground state, and the trap frequency is doubled at $t = 0$. We solve this problem by using (3.41) with $M = 30$ and time step $k = 0.001$. Figure 2 plots the condensate width and central density $|\psi(0,t)|^2$ as functions of time. Our numerical experiments also show that the scheme (3.41) with $M = 30$ gives similar numerical results as the TSSP method [10, 11] for this example with 129^2 grid points over the box $[-8, 8]^2$ and time step $k = 0.001$.

Example 3. The 3-D Gross-Pitaevskii equation with cylindrical symmetry: we choose $d = 3$, $\gamma_r = \gamma_x = \gamma_y = 4$, $\gamma_z = 1$ and $\beta_3 = 100$ in (2.9). The initial data $\psi_0(r, z)$ is chosen as the ground state of the 3-D GPE (2.9) with $d = 3$, $\gamma_r = \gamma_x = \gamma_y = 1$, $\gamma_z = 4$ and $\beta_3 = 100$ [6, 9]. This corresponds to an experimental setup where initially the condensate is assumed to be in its ground state, and at $t = 0$, we increase the radial frequency four times and decrease the axial frequency to its quarter. We solve this problem by using (3.53) with $M = 60$ and $N = 61$ and time step $k = 0.001$. Figure 3 plots the condensate widths and central density $|\psi(0,0,t)|^2$ as functions of time.

The numerical results for these three examples clearly indicated that our new methods are very efficient and accurate.

Example 4. The 3-D vector Gross-Pitaevskii equations with cylindrical symmetry for two-component BECs: we take, in (4.1) and (4.2), $m = 1.44 \times 10^{-25}$ $[kg]$, $a_{12} =$



a). b).

Figure 2: Evolution of central density and condensate width in Example 2. '—': 'exact solutions' obtained by TSSP [10] with 1029^2 grid points over a box $[-8,8]^2$; '+ + + ': Numerical results by TSLP4 (3.41) with 30 grid points on the semi-infinite interval $[0,\infty)$. a). Central density $|\psi(0,t)|^2$; b). condensate width σ_r.

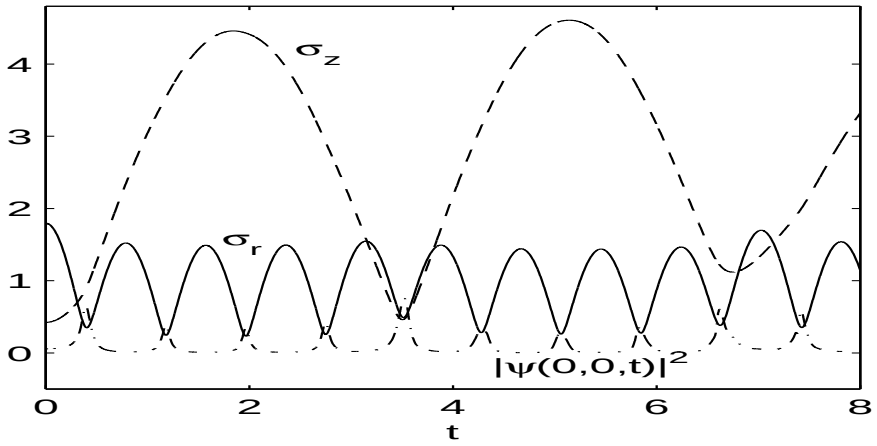
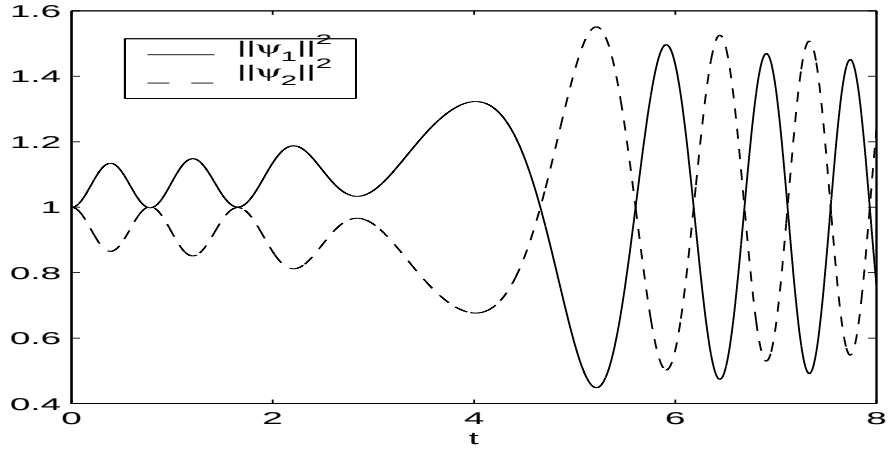


Figure 3: Evolution of central density and condensate width in Example 3 by the TSLHP4 (3.53) .

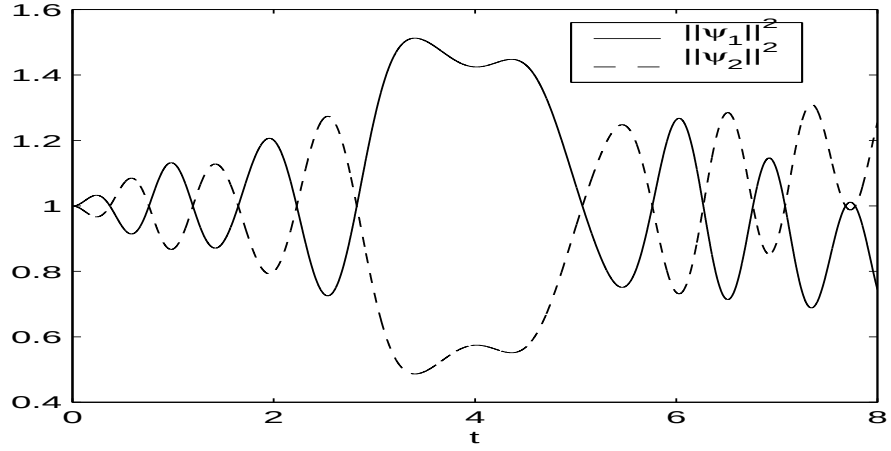
$a_{21} = 55.3\mathring{A} = 5.53\ [nm]$, $a_{11} = 1.03a_{12} = 5.6959\ [nm]$, $a_{22} = 0.97a_{12} = 5.3641\ [nm]$, $\omega_z = 47 \times 2\pi\ [1/s]$, $\omega_m = \omega_r = \omega_z/\sqrt{8}$, $N_1^0 = N_2^0 = 500,000$, $\Omega = 65 \times 2\pi\ [1/s]$, $\omega_d = 6.5 \times 2\pi\ [1/s]$. A simple computation shows $a_0 = 0.2643 \times 10^{-5}\ [m]$, $\beta_{11} = 0.02708165N_1^0$, $\beta_{12} = 0.02629286N_2^0$, $\beta_{21} = 0.02629286N_1^0$, $\beta_{22} = 0.02550407N_2^0$. The initial data $\psi_0(r,z)$ and $\phi_0(r,z)$ are chosen as the ground state of the 3-D VGPEs (4.1) and (4.2), and we set $f(t) \equiv 0$ [5]. We solve this problem by using (4.13) with $M = 100$ and $N = 201$ and time step $k = 0.00025$. Figure 4 displays the time evolution of the density functions for the two components with different trapping centers. The results are similar as those obtained in [5] by a TSSP method with a much refined grid.

¿From Fig. 4, we can see that the general form of time evolution on the number of particles in the two components is similar for different distances between the two

a).



b).



c).

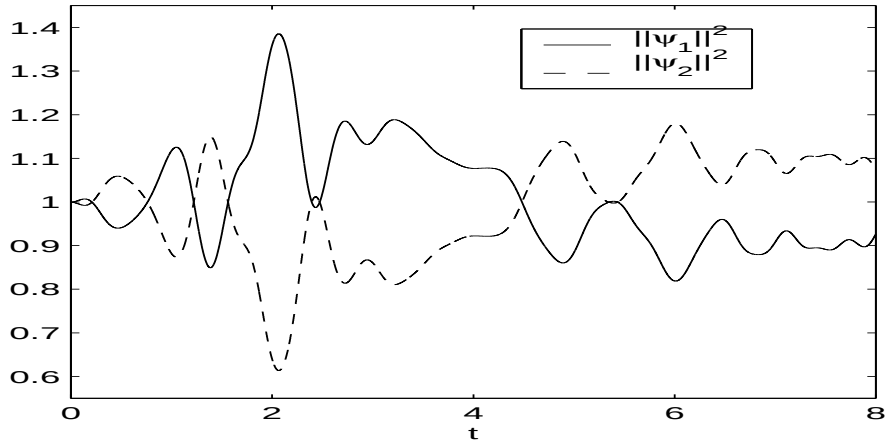


Figure 4: Time evolution of the density functions for the two-component BECs in Example 4. a). $z_1^0 = z_2^0 = 0$, b). $z_1^0 = -z_2^0 = 0.15$, c). $z_1^0 = -z_2^0 = 0.4$.

trapping potential centers. When $z_1^0 = z_2^0 = 0$, the number of particles in the second component, i.e. $N_2^0\|\phi\|^2$, decreases, reaching its bottom, oscillates and then attains its maximum at around $t = 5.2$. The number of particles in the second component at its maximum is approximately 55% bigger than its initial value at time $t = 0$. (cf. Fig. 4a). The pattern for $N_1^0\|\psi\|^2$ is exactly the opposite of that for $N_2^0\|\phi\|^2$ (cf. Fig. 4a). This antisymmetry is due to the fact that the total number of particles in the two components are conserved. When $z_1^0 - z_2^0 > 0$ becomes larger, i.e. initially the density functions for the two components are separated further, the earlier the number of particles attains its absolute peak (cf. Fig. 4b&c), the smaller the maximum of the peak is. In fact, when $z_1^0 - z_2^0 = 0.3$ (resp. 0.8), at around $t = 3.4$ (resp. 2.05), the number of particles in the first component attains its maximum which is approximately 52% (resp. 38.5%) bigger than its initial value at time $t = 0$.

6. Concluding remarks. We developed a new efficient fourth-order time-splitting Laguerre-Hermite pseudospectral method for 3-D Gross-Pitaevskii equation with cylindrical symmetry for Bose-Einstein condensates. The new method takes advantage of the cylindrical symmetry so only an effective 2-D problem is solved numerically. The new method is based on appropriately scaled Laguerre-Hermite functions and a fourth-order symplectic integrator. Hence, it is spectrally accurate in space, fourth-order accurate in time, explicit, unconditionally stable, time reversible and time transverse invariant.

When Compared with the time-splitting sine-spectral method in [10, 11, 5] and the Crank-Nicolson finite difference method in [35, 2], the new method enjoys two important advantages: (i) there is no need to truncate the original whole space into a bounded computational domain for which an artificial boundary condition (which often erodes the accuracy) is needed; (ii) it solves an effective 2-D problem instead of the original 3-D equations. Thus, the new method is very accurate and efficient, particularly in term of memory requirement. Therefore, it is extremely suitable for 3-D GPE with cylindrical symmetry which is the most frequently setup in BEC experiments. We plan to apply this powerful numerical method to study physically more complex systems like multi-component BECs, vortex states and dynamics in BECs.

REFERENCES

[1] A. Aftalion A, and Q. Du, Vortices in a rotating Bose-Einstein condensate: Critical angular velocities and energy diagrams in the Thomas-Fermi regime, Phys. Rev. A, 64(2001), pp. 063603.

[2] P. Muruganandam and S.K. Adhikari, Bose-Einstein condensation dynamics in three dimensions by the pseudospectral and finite-difference methods, J. Phys. B: At. Mol. Opt. Phys. **36**, 2501 (2003).

[3] M.H. Anderson, J.R. Ensher, M.R. Matthews, C.E. Wieman, and E.A. Cornell, Science **269**, 198 (1995).

[4] J.R. Anglin and W. Ketterle, Bose-Einstein condensation of atomic gases, Nature, 416(2002), pp. 211-218.

[5] W. Bao, Ground states and dynamics of multi-component Bose-Einstein condensates, SIAM Multiscale Modeling and Simulation, to appear (arXiv: cond-mat/0305309).

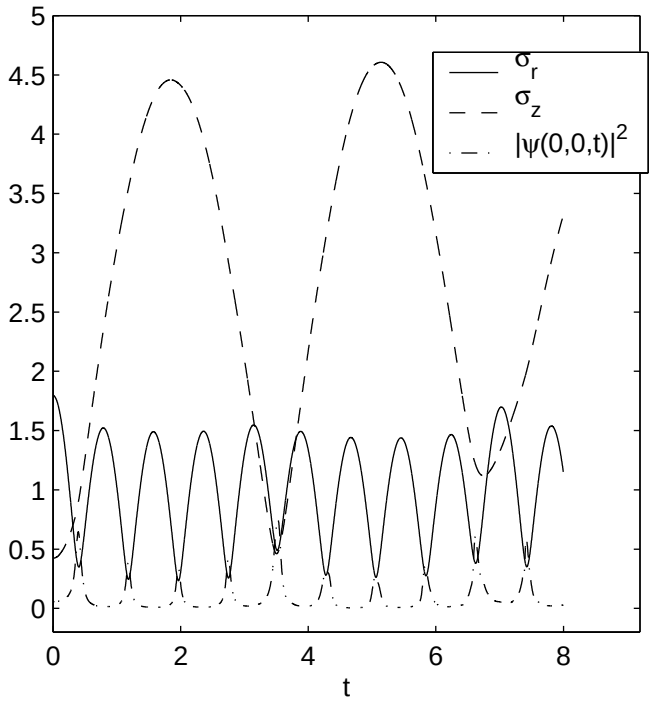
[6] W. Bao and Q. Du, Computing the ground state solution of Bose-Einstein condensates by a normalized gradient flow, SIAM J. Sci. Comp., to appear (arXiv: cond-mat/0303241).

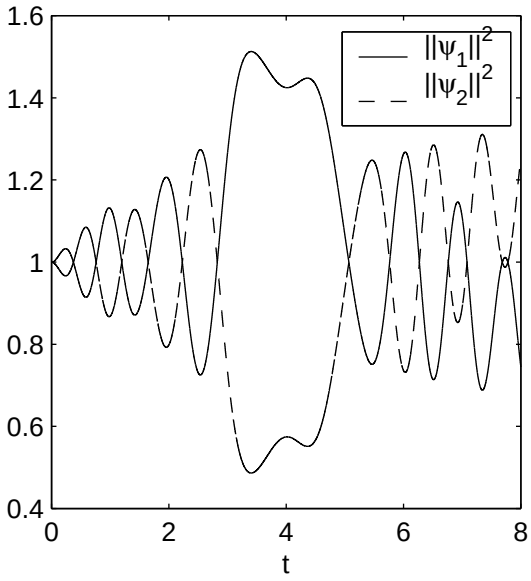
[7] W. Bao, S. Jin and P.A. Markowich, On time-splitting spectral approximations for the Schrödinger equation in the semiclassical regime, J. Comput. Phys., 175(2002), pp. 487-524.

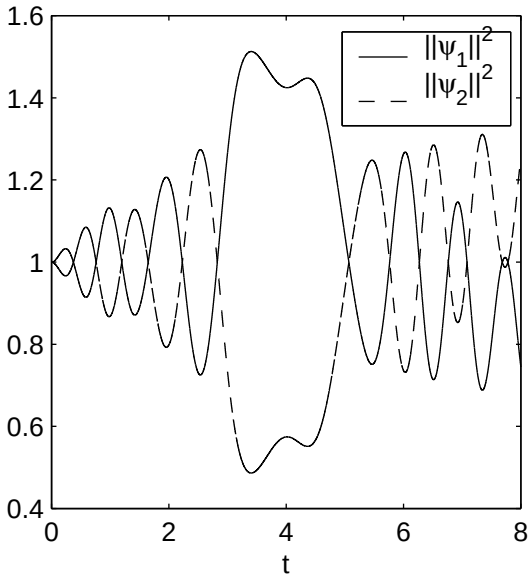
[8] W. Bao, S. Jin and P.A. Markowich, Numerical study of time-splitting spectral discretizations of nonlinear Schrödinger equations in the semi-clasical regimes, SIAM J. Sci. Comp., 25(2003), pp. 27-64.

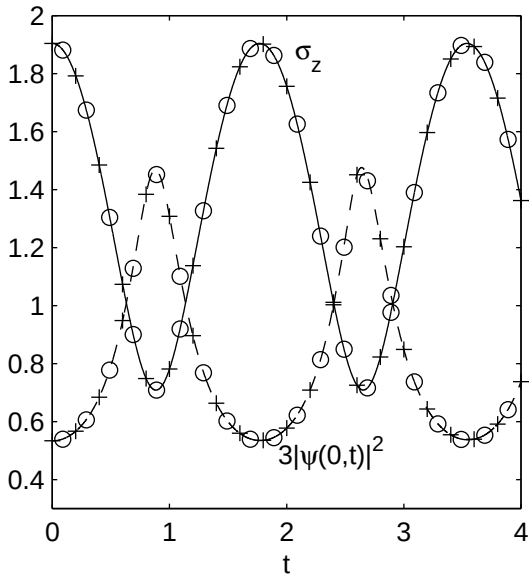
[9] W. Bao and W. Tang, Ground state solution of trapped interacting Bose-Einstein condensate by directly minimizing the energy functional, J. Comput. Phys., 187(2003), pp. 230-254.
[10] W. Bao, D. Jaksch and P.A. Markowich, Numerical solution of the Gross-Pitaevskii equation for Bose-Einstein condensation, J. Comput. Phys., 187(2003), pp. 318-342.
[11] W. Bao, D. Jaksch, An explicit unconditionally stable numerical methods for solving damped nonlinear Schrodinger equations with a focusing nonlinearity, SIAM J. Numer. Anal., 41(2003), pp. 1406-1426.
[12] G. Baym and C. J. Pethick, Phys. Rev. Lett. **76**, 6 (1996).
[13] C.C. Bradley, C.A. Sackett, R.G. Hulet, Bose-Einstein condensation of lithium: Observation of limited condensate number, Phys. Rev. Lett. 78 (1997), pp. 985-989.
[14] M.M. Cerimele, M.L. Chiofalo, F. Pistella, S. Succi and M.P. Tosi, Numerical solution of the Gross-Pitaevskii equation using an explicit finite-difference scheme: An application to trapped Bose-Einstein condensates, Phys. Rev. E, 62(2000), pp. 1382-1389.
[15] M.M. Cerimele, F. Pistella and S. succi, Particle-inspired scheme for the Gross-Pitaevski equation: An application to Bose-Einstein condensation, Comput. Phys. Comm., 129(2000), pp. 82-90.
[16] M.L. Chiofalo, S. Succi and M.P. Tosi, Ground state of trapped interacting Bose-Einstein condensates by an explicit imaginary-time algorithm, Phys. Rev. E, 62(2000), pp. 7438-7444.
[17] E. Cornell, Very cold indeed: The nanokelvin physics of Bose-Einstein condensation, J. Res. Natl. Inst. Stan. **101**, 419 (1996).
[18] F. Dalfovo S. Giorgini, L.P. Pitaevskii, and S. Stringari, Rev. Mod. Phys. **71**, 463 (1999).
[19] R.J. Dodd, Approximate solutions of the nonlinear Schrödinger equation for ground and excited states of Bose-Einstein condensates, J. Res. Natl. Inst. Stan., 101(1996), pp. 545-552.
[20] M. Edwards and K. Burnett, Numerical solution of the nonlinear Schrödinger equation for small samples of trapped neutral atoms, Phys. Rev. A **51**, 1382 (1995).
[21] M. Edwards, P.A. Ruprecht, K. Burnett, R.J. Dodd, and C.W. Clark, Phys. Rev. Lett. **77**, 1671 (1996); D.A.W. Hutchinson, E. Zaremba, and A. Griffin, Phys. Rev. Lett. **78**, 1842 (1997).
[22] D. Funaro. *Polynomial Approxiamtions of Differential Equations*. Springer-verlag, 1992.
[23] M. Greiner, O. Mandel, T. Esslinger, T.W. Hänsch, and I. Bloch, Quantum phase transition from a superfluid to a mott insulator in a gas of ultracold atoms, Nature, 415(2002), pp. 39-45.
[24] A. Griffin, D. Snoke, S. Stringaro (Eds.), Bose-Einstein condensation, Cambridge University Press, New York, 1995.
[25] E.P. Gross, Nuovo. Cimento., 20(1961), pp. 454.
[26] D.S. Hall, M.R. Mattthews, J.R. Ensher, C.E. Wieman and E.A. Cornell, Dynamics of component separation in a binary mixture of Bose-Einstein condensates, Phys. Rev. Lett., 81 (1998), pp. 1539-1542.
[27] B.-Y. Guo, J. Shen, and C.-L. Xu. Spectral and pseudospectral approximations using Hermite functions: application to the Dirac equation. *Adv. Comput. Math.*, 19(1-3):35–55, 2003. Challenges in computational mathematics (Pohang, 2001).
[28] D. Jaksch, C. Bruder, J. I. Cirac, C. W. Gardiner, and P. Zoller, Cold bosonic atoms in optical lattices, Phys. Rev. Lett., 81(1998), pp. 3108-3111.
[29] L. Laudau and E. Lifschitz, Quantum Mechanics: non-relativistic theory, Pergamon Press, New York, 1977.
[30] P. Leboeuf and N. Pavloff, Phys. Rev. A **64**, 033602 (2001); V. Dunjko, V. Lorent, and M. Olshanii, Phys. Rev. Lett. **86**, 5413 (2001).
[31] J. Lee and B. Fornberg, A split step approach for the 3-d Maxwell's equations, J. Comput. and Appl. Math., to appear.
[32] A.S. Parkins and D.F. Walls, Physics Reports **303**, 1 (1998).
[33] L.P. Pitaevskii, Vortex lines in a imperfect Bose gase, Zh. Eksp. Teor. Fiz. **40**, 646, 1961. (Sov. Phys. JETP **13**, 451, 1961).
[34] D. S. Rokhsar, Phys. Rev. Lett. **79**, 2164 (1997); R. Dum, J.I. Cirac, M. Lewenstein, and P. Zoller, Phys. Rev. Lett. 80, 2972 (1998); P. O. Fedichev, and G. V. Shlyapnikov, Phys. Rev. A **60**, R1779 (1999).
[35] P.A. Ruprecht, M.J. Holland, K. Burrett and M. Edwards, Time-dependent solution of the nonlinear Schrödinger equation for Bose-condensed trapped neutral atoms, Phys. Rev. A, 51(1995), pp. 4704-4711.
[36] B.I. Schneider and D.L. Feder, Numerical approach to the ground and excited states of a Bose-Einstein condensated gas confined in a completely anisotropic trap, Phys. Rev. A, 59(1999), pp. 22332-2242.

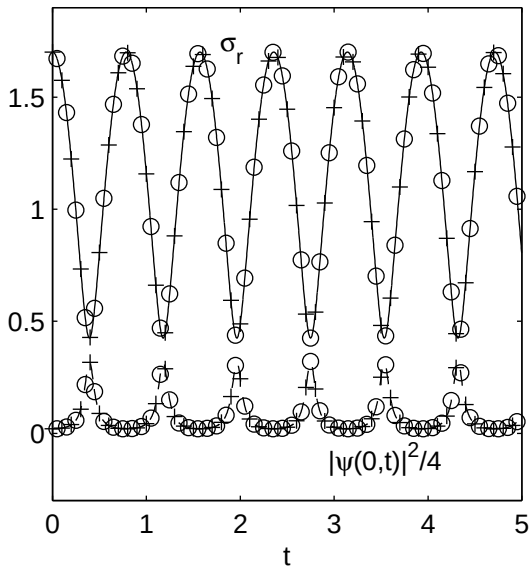
[37] J. Shen, Efficient spectral-Galerkin methods III. polar and cylindrical geometries. *SIAM J. Sci. Comput.*, 18:1583–1604, 1997.
[38] J. Shen, A new fast Chebyshev-Fourier algorithm for the Poisson-type equations in polar geometries. *Appl. Numer. Math.*, 33:183–190, 2000.
[39] G. Strang, On the construction and comparison of difference schemes. *SIAM J. Numer. Anal.*, 5:506–517, 1968.
[40] G. Szegö, *Orthogonal Polynomials (fourth edition).* AMS Coll. Publ. vol. 23, 1975.
[41] H. Yoshida, Construction of higher order symplectic integrators, Phys. Lett. A., 150(1990), pp. 262-268.


5
4.5
4
3.5
3
2.5
2
1.5
1
0.5
0
0
2
4
6
8
t
σr
σz
|ψ(0,0,t)|2


1.6
1.4
1.2
1
0.8
0.6
0.4
0
2
4
6
8
t
$\|\psi_1\|^2$
$\|\psi_2\|^2$


1.6
1.4
1.2
1
0.8
0.6
0.4
0
2
4
6
8
t
$\|\psi_1\|^2$
$\|\psi_2\|^2$


2
1.8
1.6
1.4
1.2
1
0.8
0.6
0.4
0
1
2
3
4
t
σz
3|ψ(0,t)|2


σr
1.5
1
0.5
0
|ψ(0,t)|2/4
0
1
2
3
4
5
t